Tokyo Climate Center, Japan Meteorological Agency

# TCC News

No. 48 Spring 2017

Contents



## Launch of JMA's Global Ensemble Prediction System for one-month prediction

**JMA replaced the previous One-month EPS (Ensemble Prediction System) with the Global EPS (GEPS) on Thursday 23 March 2017 to produce prediction maps and gridded datasets for one-month predictions on the TCC website. The GEPS is an integrated solution supporting JMA's issuance of typhoon information, one-week forecasts and one-month forecasts. Major changes from the previous One-month EPS and related performance are described below.**

### 1. Change in operational configuration of ensemble members from initial dates

To support the provision of one-month prediction products on the TCC website every Thursday, the GEPS is run once a week with 50 members composed of 13 members each integrated from initial fields at 00 and 12 UTC every Tuesday and Wednesday. Those of the previous One-month EPS were composed of 25 members each integrated from initial fields at 12 UTC every Tuesday and Wednesday. In terms of gridded dataset dissemination for one-month prediction, the 50 members will be composed of a 24-member set (Tuesday) and a 26-member set (Wednesday) as of Thursday 23 March 2017 based on this operational configuration change.

### 2. Major updates

Major changes in the new GEPS compared with the previous One-month EPS are as follows:

- Atmospheric global circulation model (AGCM)
  - » A low-resolution version of JMA's Global Spectral Model (GSM) launched in March 2016 (GSM1603) is used with additional improvement of physical processes.
  - » Horizontal resolution has been increased from TL319 (55 km) to TL479 (40 km) from the initial time up to 18 days ahead, whereas the resolution from the 18th day on is the same as that of the previous system (i.e., TL319 (55 km)).
  - » The number of vertical layers has been increased from 60 to 100, and the pressure of the top level has been increased from 0.1 to 0.01 hPa.
- Ensemble method
  - » A combination of the Local Ensemble Transform Kalman Filter (LETKF) method and the Singular Vector (SV) methods has been introduced to produce initial perturbation as an alternative to the Breeding Growing Mode (BGM) method.
  - » Sea surface temperature perturbation has been introduced for production of boundary conditions.

### 3. Performance

In advance of the upgrade, a full set of hindcast experiments for the 32-year period from 1981 to 2012 was executed using the new system. Atmospheric initial conditions for the experiments were taken from the Japanese 55-year Reanalysis (JRA-55, Kobayashi et al. 2015), which is an advanced dataset produced by JMA. Verification of the hindcast for the 30-year period from 1981 to 2010 indicates prediction skill enhancement. By way of example, the forecast mean error of the weak Asian monsoon in summer became smaller than that of the previous One-month EPS in terms of velocity potential at 200 hPa (Figure 1), and anomaly correlation coefficients of geopotential height at 500 hPa over the Northern Hemisphere for all seasons (Figure 2) show improvement under the new system.

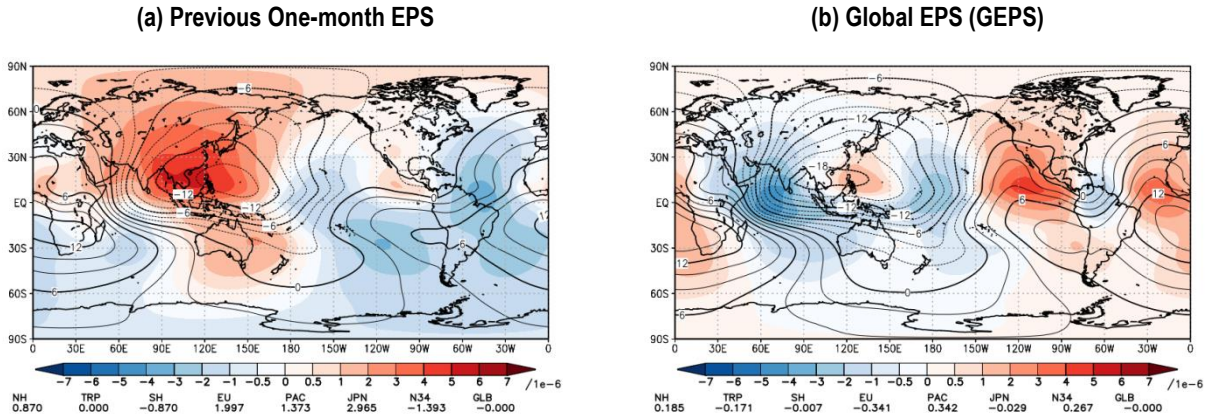


**Figure 1 Climatological fields of velocity potential at 200 hPa (contours) and related mean error (shading) for summer with (a) the previous One-month EPS and (b) the Global EPS (GEPS)**
The contour interval is $2 \times 10^6$ $m^2/s$.

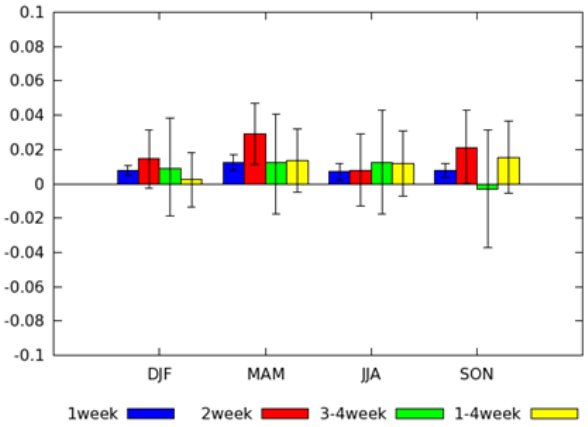


**Figure 2 Differences in anomaly correlation coefficients for one-month mean geopotential height at 500 hPa**
Positive values represent GEPS anomaly correlation coefficients greater than those of the previous One-month EPS. Higher values indicate more accurate forecasts.

Products for one-month forecasting are available on the TCC website:
http://ds.data.jma.go.jp/tcc/tcc/products/model/index.html.

*(Shiro Ishizaki, Climate Prediction Division)*

**References:**

Kobayashi, S., Y. Ota, Y. Harada, A. Ebita, M. Moriya, H. Onoda, K. Onogi, H. Kamahori, C. Kobayashi, H. Endo, K. Miyaoka, and K. Takahashi, 2015: The JRA-55 reanalysis: General specifications and basic characteristics. *J. Meteor. Soc. Japan*, **93**, 5-48.

# El Niño Outlook (May 2017 – November 2017)

**There is a 50% probability that an El Niño event will emerge by the beginning of boreal autumn. (Article based on the El Niño outlook issued on 12 May 2017.)**

**El Niño/La Niña**

The NINO.3 SST deviation was +0.6°C in April, having remained at +0.5°C or more since February. SSTs in April were above normal in much of the equatorial Pacific except near the date line, where below-normal values were observed (Figures 3 and 5(a)). Subsurface temperatures were above normal in the western equatorial Pacific and below normal in the central part (Figures 4 and 5(b)). Atmospheric convective activity was below normal near the date line over the equatorial Pacific, and easterly winds in the lower troposphere (trade winds) were near normal over the central part. In summary, despite the recent persistence of above-normal NINO.3 SSTs, no clear signs of El Niño development were observed in April.

JMA's El Niño prediction model suggests that the NINO.3 SST will be above or near normal during the prediction period (Figure 6). Based on this prediction and the observations detailed above, there is a 70% likelihood that the five-month running mean NINO.3 SST in April will be +0.5°C or above. However, there is a probability of around 50% that this value will persist in boreal summer and beyond (Figure 7). In conclusion, there is a 50% probability that an El Niño event will emerge by the beginning of boreal autumn.

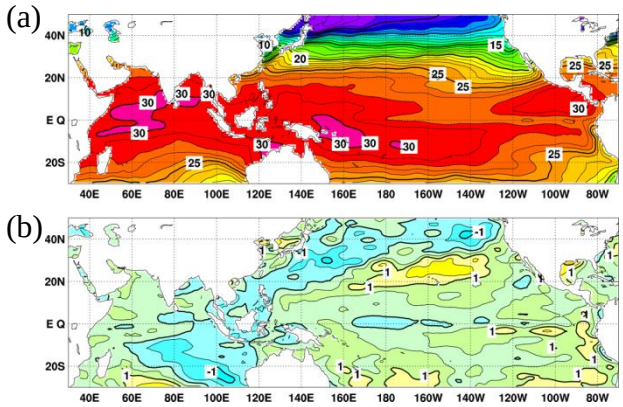


**Figure 3 Monthly mean (a) sea surface temperatures (SSTs) and (b) SST anomalies in the Indian and Pacific Ocean areas for April 2017**

The contour intervals are 1˚C in (a) and 0.5˚C in (b). The base period for the normal is 1981 – 2010.

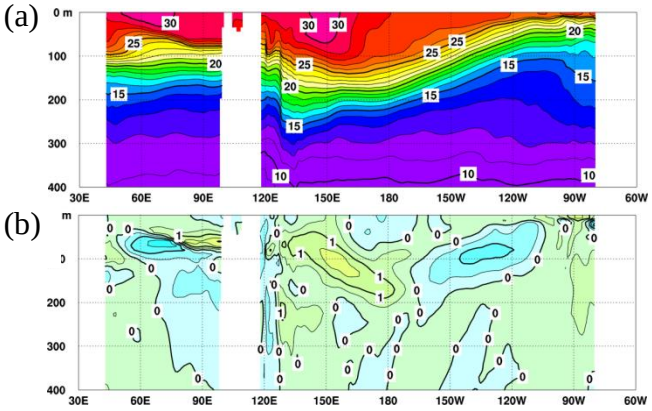


**Figure 4 Monthly mean depth-longitude cross sections of (a) temperatures and (b) temperature anomalies in the equatorial Indian and Pacific Ocean areas for April 2017**

The contour intervals are 1˚C in (a) and 0.5˚C in (b). The base period for the normal is 1981 – 2010.

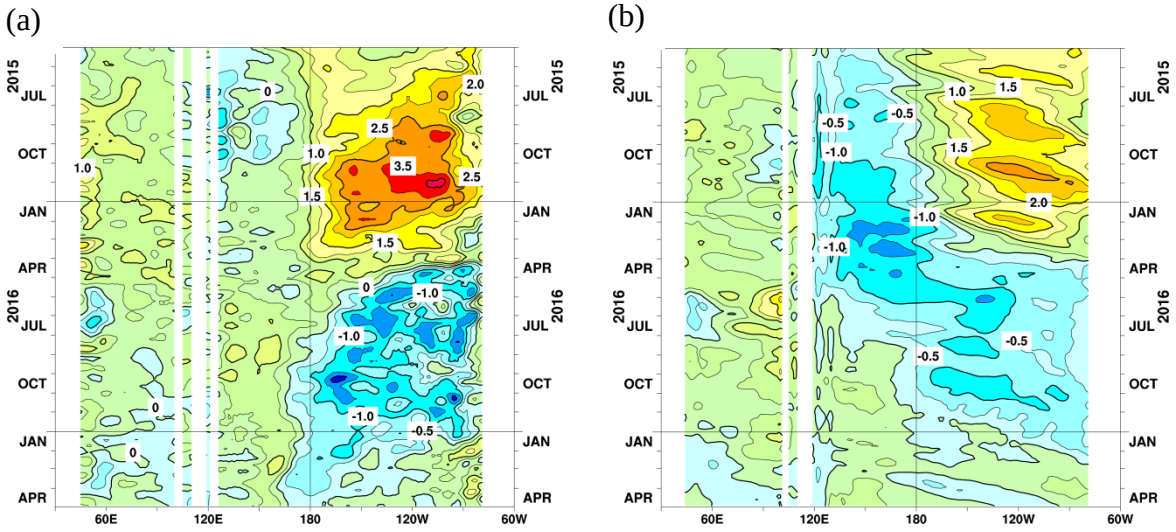


**Figure 5 Time-longitude cross sections of (a) SST and (b) ocean heat content (OHC) anomalies along the equator in the Indian and Pacific Ocean areas**

OHCs are defined here as vertical averaged temperatures in the top 300 m. The base period for the normal is 1981 – 2010.

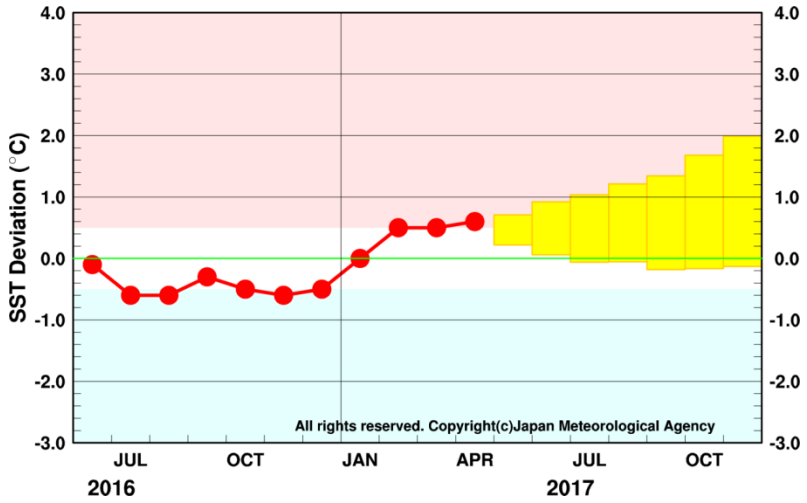


**Figure 6 Outlook of NINO.3 SST deviation produced by the El Niño prediction model**
This figure shows a time series of monthly NINO.3 SST deviations. The thick line with closed circles shows observed SST deviations, and the boxes show the values produced for up to six months ahead by the El Niño prediction model. Each box denotes the range into which the SST deviation is expected to fall with a probability of 70%.

| YEAR | MONTH | mean period | | |
|---|---|---|---|---|
| | MAR | JAN2017–MAY2017 | 20 | 80 |
| | APR | FEB2017–JUN2017 | 70 | 30 |
| | **MAY** | **MAR2017–JUL2017** | 60 | 40 |
| 2017 | **JUN** | **APR2017–AUG2017** | 50 | 50 |
| | **JUL** | **MAY2017–SEP2017** | 50 | 50 |
| | **AUG** | **JUN2017–OCT2017** | 50 | 50 |
| | **SEP** | **JUL2017–NOV2017** | 50 | 50 |

El Niño ENSO neutral La Niña

**Figure 7 ENSO forecast probabilities based on the El Niño prediction model**
Red, yellow and blue bars indicate probabilities that the five-month running mean of the NINO.3 SST deviation from the latest sliding 30-year mean will be +0.5°C or above (El Niño), between +0.4 and -0.4°C (ENSO-neutral) and -0.5°C or below (La Niña), respectively. Regular text indicates past months, and bold text indicates current and future months.

**Western Pacific and Indian Ocean**

The area-averaged SST in the tropical western Pacific (NINO.WEST) region was near normal in April. It is likely that the values will remain near normal until boreal summer.

The area-averaged SST in the tropical Indian Ocean (IOBW) region was below normal in April. It is likely that the values will gradually approach the normal toward boreal summer.

*(Ichiro Ishikawa, Climate Prediction Division)*

* The SST normal for the NINO.3 region (5°S – 5°N, 150°W – 90°W) is defined as a monthly average over the latest sliding 30-year period (1986-2015 for this year).
* The SST normals for the NINO.WEST region (Eq. – 15°N, 130°E – 150°E) and the IOBW region (20°S – 20°N, 40°E – 100°E) are defined as linear extrapolations with respect to the latest sliding 30-year period, in order to remove the effects of significant long-term warming trends observed in these regions.

# JMA's Seasonal Numerical Ensemble Prediction for Boreal Summer 2017

**Based on JMA's seasonal ensemble prediction system, sea surface temperature (SST) anomalies are predicted to be above normal in the equatorial Pacific during this boreal summer, suggesting El Niño-like conditions. Active convection is predicted over the sea east of New Guinea, while inactive convection is predicted over the western Indian Ocean. Precipitation is predicted to be above normal over and around the Indochina Peninsula and the Philippines, reflecting an active Southeast Asian Monsoon.**

## 1. Introduction

This article outlines JMA's dynamical seasonal ensemble prediction for boreal summer 2017 (June – August, referred to as JJA), which was used as a basis for JMA's operational warm-season outlook issued on 24 May 2017. The outlook is based on the seasonal ensemble prediction system of the Coupled Atmosphere-ocean General Circulation Model (CGCM). See the column below for system details.

Section 2 outlines global SST anomaly predictions, and Section 3 describes the associated circulation field predictions for the tropics and sub-tropics. Finally, the circulation fields predicted for the mid- and high latitudes of the Northern Hemisphere are discussed in Section 4.

## 2. SST anomalies (Figure 8)

Figure 8 shows predicted SSTs (contours) and related anomalies (shading) for JJA. Above-normal anomalies are predicted in the equatorial Pacific, suggesting El Niño-like conditions. Conversely, below-normal anomalies are predicted in some parts of the southern Indian Ocean and the Maritime Continent.

## 3. Prediction for the tropics and sub-tropics (Figure 9)

Figure 9 (a) shows predicted precipitation (contours) and related anomalies (shading) for JJA. Large above-normal anomalies are predicted over the sea east of New Guinea in association with high SSTs exceeding 30°C. Above-normal anomalies are also predicted over and around the Indochina Peninsula and the Philippines, reflecting an active Southeast Asian Monsoon. Meanwhile, below-normal anomalies are predicted over the southeastern Indian Ocean in association with low SSTs.

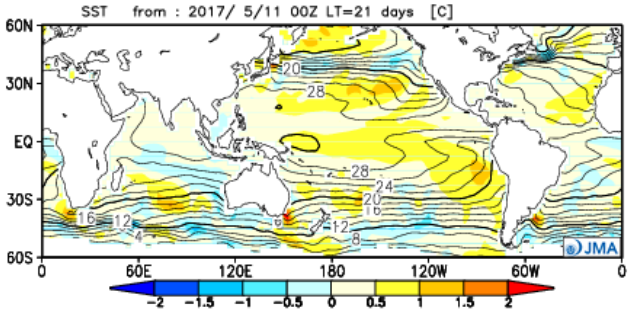


**Figure 8 Predicted SSTs (contours) and SST anomalies (shading) for June–August 2017 (ensemble mean of 51 members)**

Figure 9 (b) shows predicted velocity potential (contours) and related anomalies (shading) at the upper troposphere (200 hPa) for JJA. Negative (i.e., divergent) anomalies are predicted over the sea east of New Guinea in association with heavy precipitation. Conversely, positive (i.e., convergent) anomalies are predicted over the western Indian Ocean.

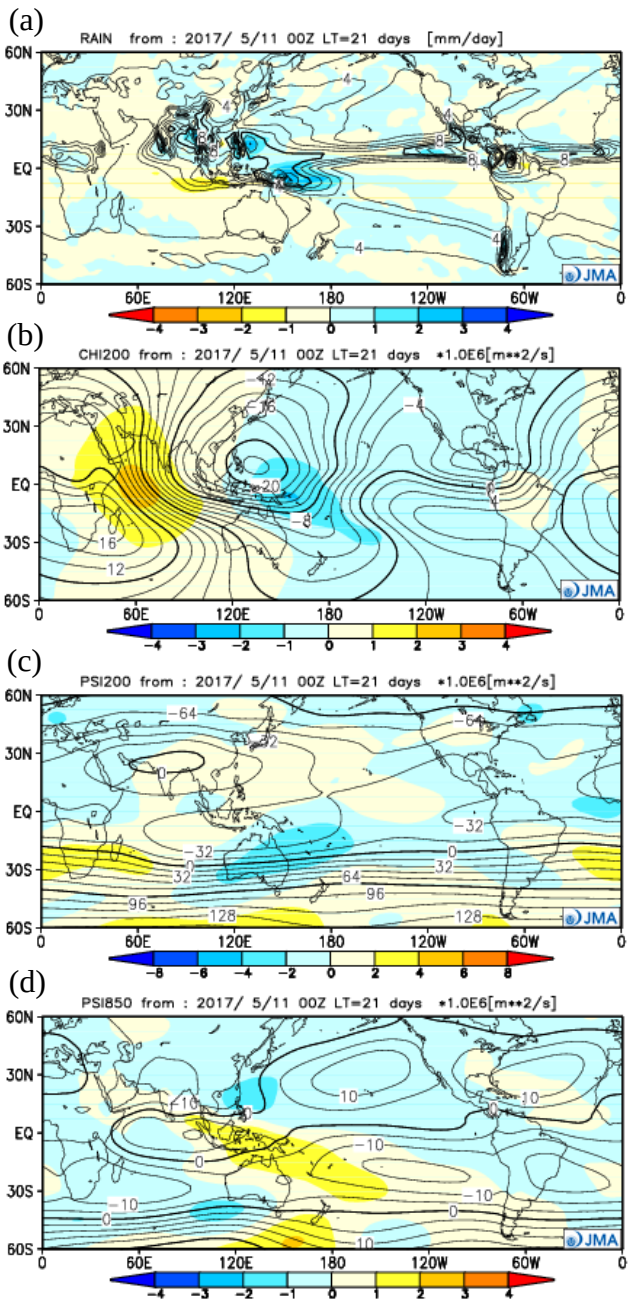


**Figure 9 Predicted atmospheric fields from 60°N – 60°S for June–August 2017 (ensemble mean of 51 members)**
(a) Precipitation (contours) and anomaly (shading). The contour interval is 2 mm/day.
(b) Velocity potential at 200 hPa (contours) and anomaly (shading). The contour interval is $2 \times 10^6$ m$^2$/s.
(c) Stream function at 200 hPa (contours) and anomaly (shading). The contour interval is $16 \times 10^6$ m$^2$/s.
(d) Stream function at 850 hPa (contours) and anomaly (shading). The contour interval is $5 \times 10^6$ m$^2$/s.

Figure 9 (c) shows predicted stream functions (contours) and related anomalies (shading) at the upper troposphere (200 hPa) for JJA. Positive (i.e., anticyclonic) anomalies are predicted over the northwestern Pacific in association with active convection over the sea east of New Guinea. Such anomalies are also predicted over China, the Indochina Peninsula and the Philippines in association with an active Southeast Asian Monsoon, suggesting a more dominant Tibetan High than normal over these regions. Conversely, negative (i.e., cyclonic) anomalies are predicted over West Asia in association with inactive convection in the western Indian Ocean.

Figure 9 (d) shows predicted stream functions (contours) and related anomalies (shading) at the lower troposphere (850 hPa) for JJA. Negative (i.e., cyclonic) anomalies are predicted over the sea north of the Philippines in association with an active Southeast Asian Monsoon. Conversely, equatorial symmetric anticyclonic anomalies are predicted over the western Indian Ocean in association with inactive convection.

**4. Prediction for the mid- and high- latitudes of the Northern Hemisphere**

Figure 10 (a) shows predicted geopotential heights (contours) and related anomalies (shading) at 500 hPa for JJA. Positive anomalies are predicted over most of the Northern Hemisphere, reflecting high thickness caused by El Niño-like conditions and global warming trends.

Figure 10 (b) shows predicted sea level pressure (contours) and related anomalies (shading) for JJA. Positive anomalies are predicted over the main islands of Japan, suggesting a more dominant North Pacific High than normal. Conversely, negative anomalies are predicted over the sea north of the Philippines, suggesting active tropical cyclones in this region.

*(Takashi Yamada, Climate Prediction Division)*

(a)

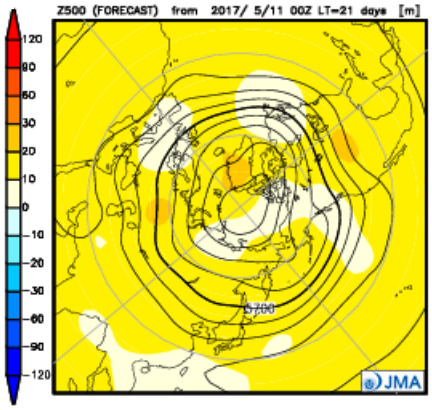


(b)

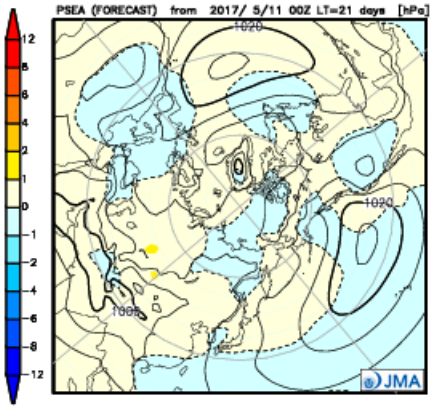


**Figures 10 Predicted atmospheric fields from 20°N – 90°N for June–August 2017 (ensemble mean of 51 members)**
(a) Geopotential height at 500hPa (contours) and anomaly (shading). The contour interval is 60 m.
(b) Sea level pressure (contours) and anomaly (shading). The contour interval is 4hPa.

**JMA's Seasonal Ensemble Prediction System**

JMA operates a seasonal Ensemble Prediction System (EPS) using the Coupled atmosphere-ocean General Circulation Model (CGCM) to make seasonal predictions beyond a one-month time range. The EPS produces perturbed initial conditions by means of a combination of the initial perturbation method and the lagged average forecasting (LAF) method. The prediction is made using 51 members from the latest four initial dates (13 members are run every 5 days). Details of the prediction system and verification maps based on 30-year hindcast experiments (1981–2010) are available at http://ds.data.jma.go.jp/tcc/tcc/products/model/.

# Warm Season Outlook for Summer 2017 in Japan

**JMA issued warm season outlook for the coming summer (June – August) over Japan in February and updated it on 24 May. This article outlines the update.**

## 1. Outlook summary (Figure 11)

- Seasonal mean temperatures are expected to be above normal all over Japan.
- Seasonal precipitation amounts are expected to be above normal on the Pacific side of western Japan and near normal in other regions of the country.

## 2. Outlook background

Figure 12 summarizes expected large-scale oceanic/atmospheric characteristics for the coming summer. The grounds for the outlook are given below.

### (1) Outlook on oceanic conditions

- Sea surface temperatures (SSTs) are expected to be higher than normal in the western tropical Pacific, especially east of New Guinea.
- SST anomalies in the tropical Indian Ocean are expected to be relatively low.

### (2) Outlook on atmospheric circulation fields

- In response to the above SST anomaly patterns, convection is expected to be more active in the western tropical Pacific with southerly shifting compared to the climatology and less active in the tropical Indian Ocean.
- In association with inactive convection in the tropical Indian Ocean, the Tibetan High is expected to be weaker than normal, and its northeastward expansion (i.e., that extending into Japan) is also expected to be weak. Accordingly, the subtropical jet stream, which flows along the northern edge of the Tibetan High, is expected to shift southward of its normal position.
- In the pre-midsummer Baiu season, the north Pacific High is expected to expand westward (i.e., to be stronger than normal over the sea south of Japan's main island) due to active and southerly shifted convection in the western tropical Pacific. Accordingly, the Baiu front will be enhanced due to moist southerly flows along the edge of the High, which could bring wet conditions to the Pacific side of western Japan and elsewhere.
- In midsummer, sea level pressure anomalies are expected to be negative south of Japan in association with active convection near the Philippines. Accordingly, the North Pacific High is expected to be stronger than normal near the country's main island (a phenomenon known as the Pacific-Japan (PJ) teleconnection pattern).
- Overall temperatures in the troposphere are expected to be higher than normal in association with the prevailing long-term trend. These tendencies are likely to increase the chances of above-normal temperatures.

*(Masayuki Hirai, Climate Prediction Division)*

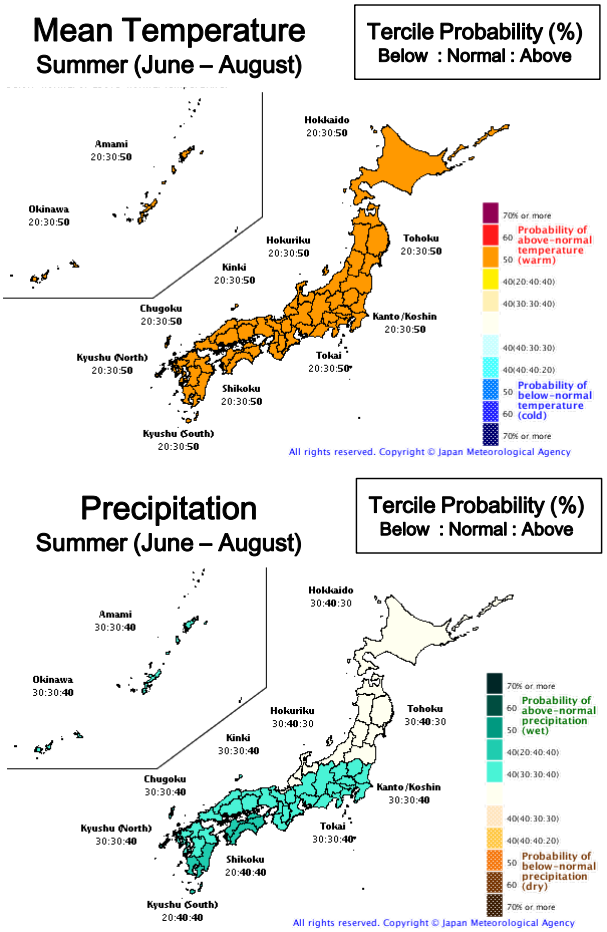


**Figure 11: Outlook for summer 2017 temperature (top) and precipitation (bottom) probability in Japan**

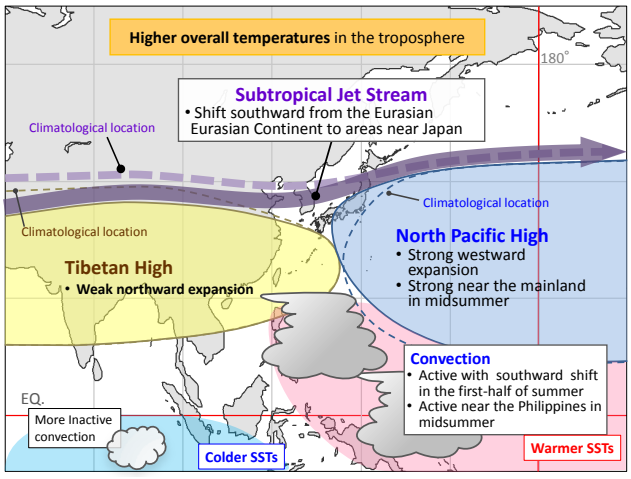


**Figure 12: Conceptual diagram showing expected large-scale ocean/atmosphere characteristics for summer 2017**

# Summary of the 2016/2017 Asian Winter Monsoon

**This report summarizes the characteristics of the surface climate and atmospheric/oceanographic considerations related to the Asian winter monsoon for 2016/2017.**

Note: The Japanese 55-year Reanalysis (JRA-55; Kobayashi et al. 2015) atmospheric circulation data and COBE-SST (Ishii et al. 2005) sea surface temperature (SST) data were used for this investigation. The outgoing longwave radiation (OLR) data referenced to infer tropical convective activity were originally provided by NOAA. The base period for the normal is 1981 – 2010. The term "anomaly" as used in this report refers to deviation from the normal.

## 1. Surface climate conditions

Most Asian countries experienced warmer-than-normal conditions throughout boreal winter 2016/2017 (Figure 13). Three-month mean temperatures for December 2016 – February 2017 were ranked as very warm across large areas of China, Southeast Asia and western India. Precipitation amounts during the season were above normal in northeastern China, Central Asia, Southeast Asia and Micronesia, and below normal in southwestern China and northern India (Figure 14).

Figure 15 shows extreme climate events occurring between December 2016 and February 2017. In December, extremely high temperatures were seen in many parts of Mongolia, China, India, Sri Lanka and Pakistan, and extremely high precipitation amounts were observed around the Korean Peninsula. In January, extremely high temperatures were seen over southern China and northern Myanmar, and extremely high precipitation amounts were observed from the southern Indochina Peninsula to northern Sumatra Island. In southern Thailand, more than 90 casualties due to heavy rain were reported in January (European Commission). Precipitation for January at Songkhla in southern Thailand was 682 mm (776% of the 1981 – 2010 normal) according to CLIMAT reports. In February, extremely high temperatures were seen from the southern part of Eastern Siberia to the southeastern part of Central Siberia.

Although most of the season was warmer than normal, cold-air outbreaks were recorded over many parts of East Asia in mid-January and early February (Figure 16), bringing heavy snowfall to the Sea of Japan side of western Japan.

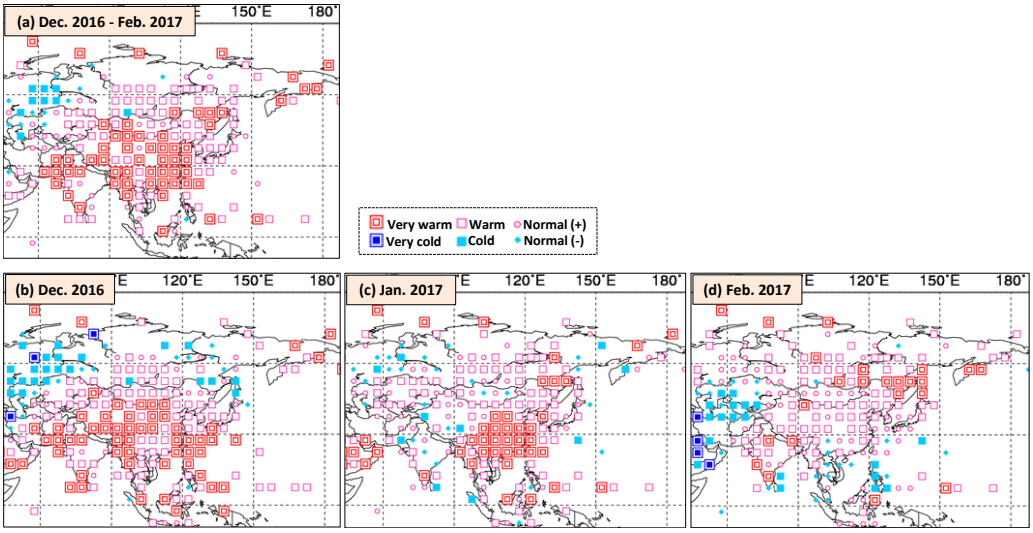


**Figure 13 (a) Three-month mean temperature anomalies for December 2016 – February 2017, and monthly mean temperature anomalies for (b) December 2016, (c) January 2017 and (d) February 2017**
Categories are defined by the three-month/monthly mean temperature anomaly against the normal divided by its standard deviation and averaged in 5° × 5° grid boxes. The thresholds of each category are -1.28, -0.44, 0, +0.44 and +1.28. Standard deviations were calculated from 1981 - 2010 statistics. Areas over land without graphical marks are those where observation data are insufficient or where normal data are unavailable.

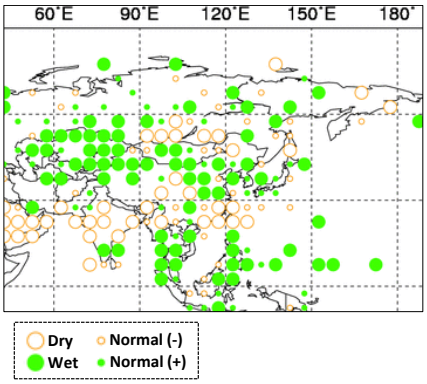


**Figure 14 Three-month total precipitation ratio for December 2016 – February 2017**
Categories are defined by the three-month mean precipitation ratio against the normal and averaged in 5° × 5° grid boxes. The thresholds of each category are 70, 100 and 120%. Areas over land without graphical marks are those where observation data are insufficient or where normal data are unavailable.

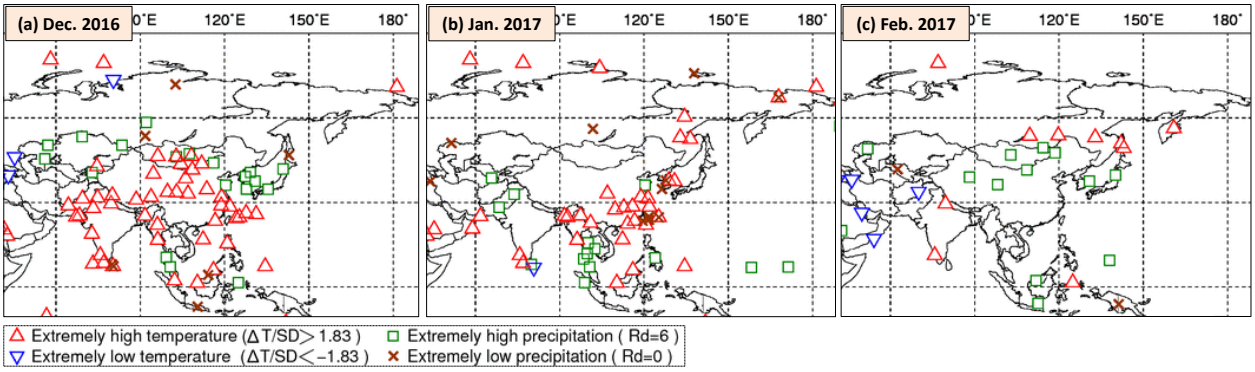


**Figure 15 Extreme climate events for (a) December 2016, (b) January 2017 and (c) February 2017**
ΔT, SD and Rd indicate temperature anomaly, standard deviation and quintile, respectively.

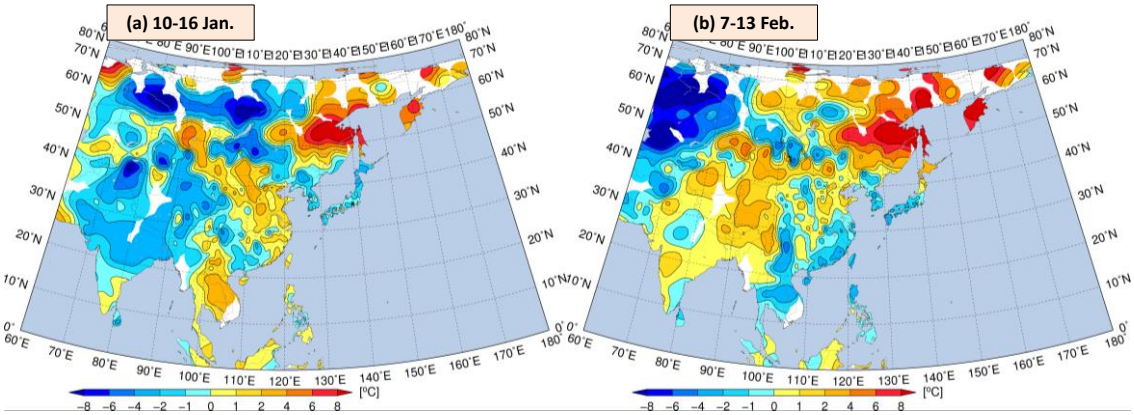


**Figure 16 Seven-day surface temperature anomalies for (a) 10 – 16 January and (b) 7 – 13 February 2017.**
Both are based on SYNOP observation data.

## 2. Characteristic atmospheric circulation and oceanographic conditions

### 2.1 Conditions in the tropics

In winter 2016/2017, sea surface temperatures (SSTs) along the equator were above normal in the western Pacific and below normal in the central – eastern Pacific (Figure 17). SSTs over the South China Sea to the seas east of the Philippines were higher than normal.

Convective activity inferred from outgoing longwave radiation (OLR) during the season was enhanced in Southeast Asia and suppressed over the Indian Ocean and the equatorial Pacific (Figure 18 (a)). In Southeast Asia, where precipitation during this winter was generally categorized as above normal (Figure 14), enhanced convection remained throughout the season, especially over the Indochina and Malay peninsulas in December (Figure 18 (b)) and January (Figure 18 (c)).

In the upper troposphere, clear large-scale divergent anomalies were seen over Southeast Asia in association with enhanced convective activity, and convergent anomalies were observed over the Indian Ocean and the Pacific (Figure 19 (a)). In the stream function field (Figure 19 (b)), anticyclonic circulation anomalies were centered over southeastern China.

In the lower troposphere, a pair of cyclonic circulation anomalies was observed along the equator over the area from the eastern Indian Ocean to the Maritime Continent (Figure 19 (c)). In early January, a cyclonic circulation system with enhanced convection brought heavy rain to southern Thailand (Figure 20).

An active convection phase of the Madden-Julian Oscillation (MJO) propagated eastward globally from the latter half of January to February (Figure 21 (a)). Southern Oscillation Index values remained near normal during winter.

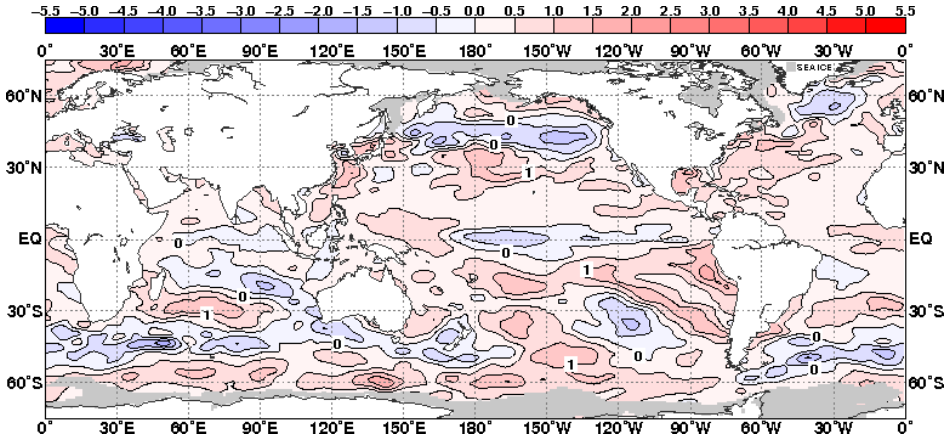

**Figure 17 Three-month mean sea surface temperature (SST) anomalies for December 2016 to February 2017**
The contour interval is 0.5˚C.

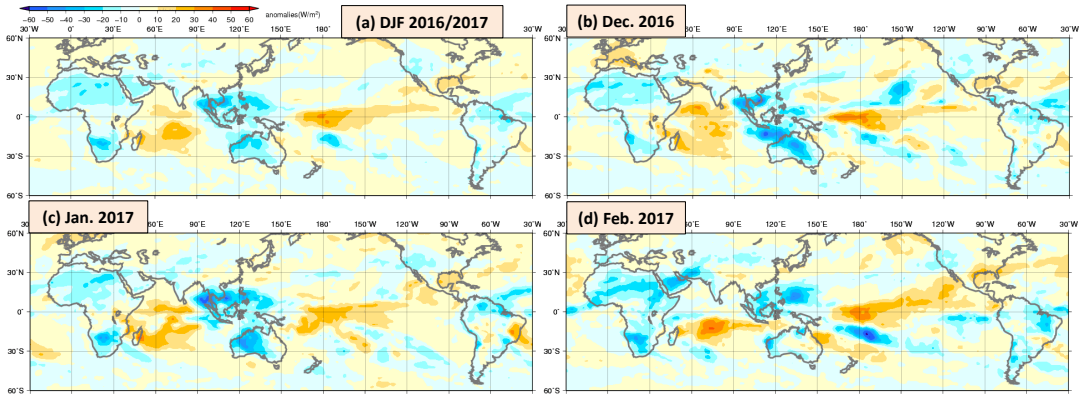


**Figure 18 Outgoing longwave radiation (OLR) anomalies (a) averaged over the three months from December 2016 to February 2017, and for (b) December 2016, (c) January 2017 and (d) February 2017.**
Blue and red shading indicates areas of enhanced and suppressed convective activity, respectively.

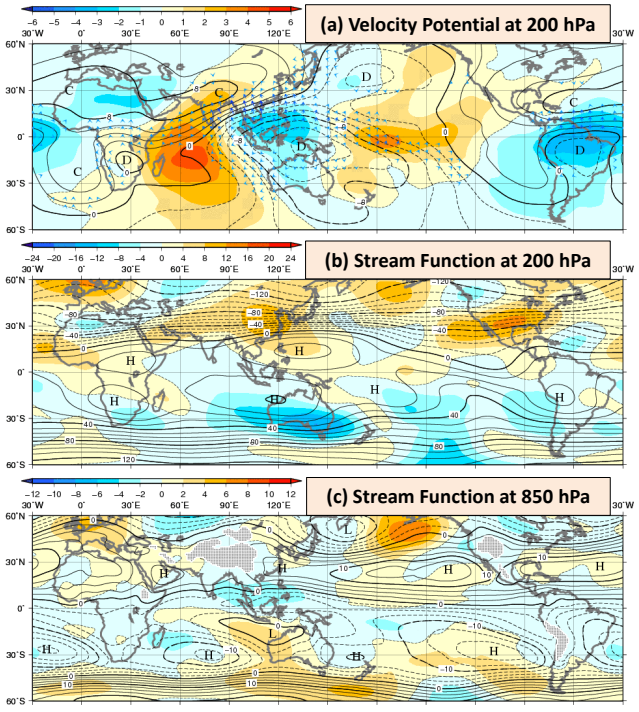


**Figure 19 Three-month mean (a) 200-hPa velocity potential, (b) 200-hPa stream function, and (c) 850-hPa stream function for December 2016 to February 2017 (unit: 106 m2/s)**
(a) The contours indicate velocity potential at intervals of $2 \times 10^6$ $m^2/s$, and the shading shows velocity potential anomalies. D and C indicate the bottom and the peak of velocity potential, corresponding to the centers of large-scale divergence and convergence, respectively. (b, c) The contours indicate stream function at intervals of (b) 10 and (c) $2.5 \times 10^6$ $m^2/s$, and the shading shows stream function anomalies. H and L denote the centers of anticyclonic and cyclonic circulations, respectively.

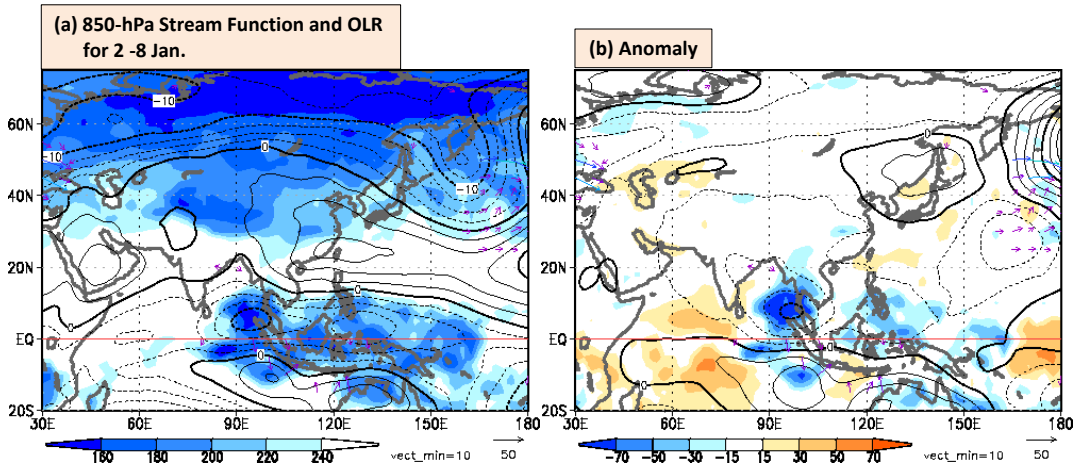


**Figure 20 (a) Seven-day mean 850-hPa stream function (contours) and outgoing longwave radiation (OLR; shading) for 2 – 8 January 2017, and (b) related anomaly**

The thin and thick contour intervals are 2.5 and 10 × $10^6$ $m^2/s$, respectively. Lower OLR values indicate enhanced convective activity except in the mid- and high latitudes. The blue and red shading in (b) indicates areas of enhanced and suppressed convective activity, respectively. Arrows show wave activity fluxes indicating Rossby wave packet propagation.

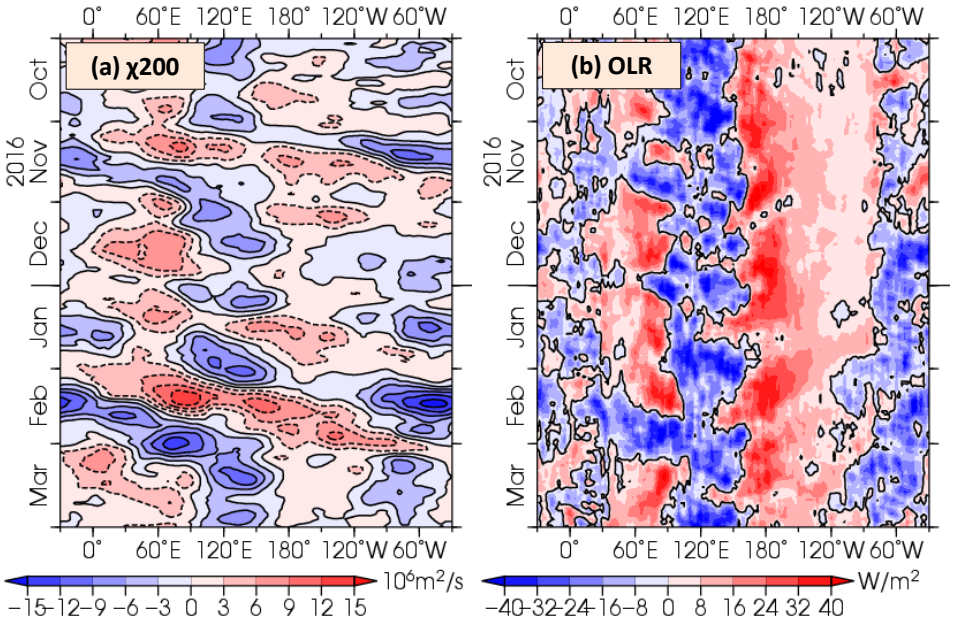


**Figure 21 Time-longitude cross section of seven-day running mean (a) 200-hPa velocity potential anomalies, and (b) outgoing longwave radiation (OLR) anomalies around the equator (5°S – 5°N) for October 2016 to March 2017**

(a) The blue and red shading indicates areas of divergence and convergence anomalies, respectively. (b) The blue and red shading indicates areas of enhanced and suppressed convective activity, respectively.

### 2.2 Conditions in the extra-tropics and the Asian Winter Monsoon

In the 500-hPa height field in winter 2016/2017 (Figure 22 (a)), wave trains were seen along the subpolar jet stream over the Eurasian Continent with positive anomalies in northern Europe and northern East Asia, and negative anomalies in Western Siberia and over the seas to the east of Japan. In the sea level pressure field (Figure 23 (a)), the Aleutian Low was centered to the west of its normal position. The Siberian High was generally weaker than normal, indicating that the Asian Winter Monsoon was not as active as in normal winters.

Over East Asia, tropospheric temperatures were higher than normal (Figure 24) due to the northward meandering of the subpolar jet stream over northern East Asia (Figure 22 (a)) and the subtropical jet stream over southern China (Figure 19 (b)), causing warmer-than-normal winter conditions (Figure 13).

The subpolar jet stream meandered southward over Western Siberia (Figure 22 (a)), where negative sea level pressure anomalies were also centered (Figure 23 (a)). This pattern brought southerly warm winds to Siberia and appears to have prohibited Siberian High development.

Figure 25 shows that the intraseasonal variability of the Siberian High generally coincides with that of 500-hPa height over Western Siberia. This weaker-than-normal Siberian High was another factor behind the warm conditions seen in East Asia.

In the first half of winter, southerly wind anomalies prevailed over southern China (Figure 26), where extreme high temperatures were observed in December and January (Figure 15) in association with cyclonic circulation anomalies around Southeast Asia and anticyclonic circulation anomalies to the east of Japan. Northerly cold air flowed into the region less frequently than in normal winters, which contributed to the extreme high temperatures observed over southern China.

As mentioned above, temperatures in mid-January and early February over many parts of East Asia dropped significantly (Figure 16), and heavy snowfall was observed in Japan. During these periods, blocking highs developed around the Bering Sea and migrated westward to Eastern Siberia, and troughs deepened to the south of these highs (Figures 27 (a), (d)). In the sea level pressure fields (Figures 27 (b), (e)), the Siberian High extended to the eastern coast of the Eurasian Continent and the Aleutian Low also intensified, bringing strong cold-air flow into East Asia (Figures 27 (c), (f)).

*(Hiroshi Ohno, Climate Prediction Division)*

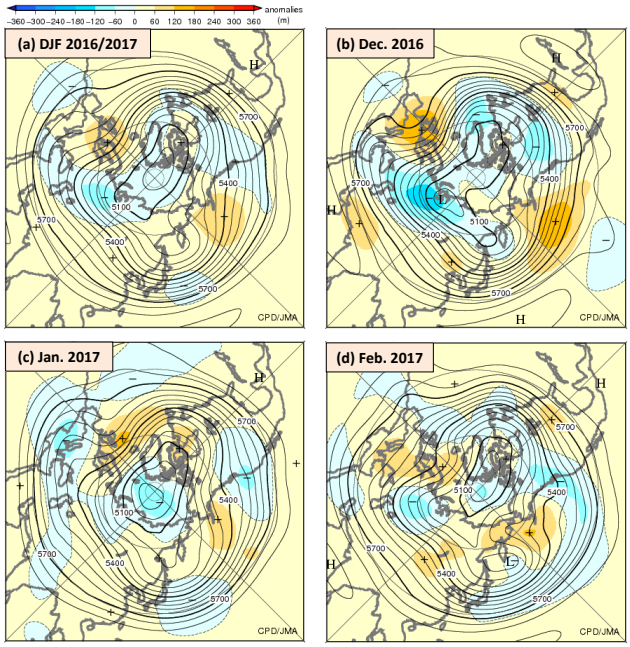


**Figure 22 500-hPa height (a) averaged over the three months from December 2016 to February 2017, for (b) December 2016, (c) January 2017, and (d) February 2017**

The contours indicate 500-hPa height at intervals of 60 m, and the shading denotes anomalies. H and L indicate the peak and bottom of 500-hPa height, respectively, and + (plus) and – (minus) show the peak and bottom of anomalies, respectively.

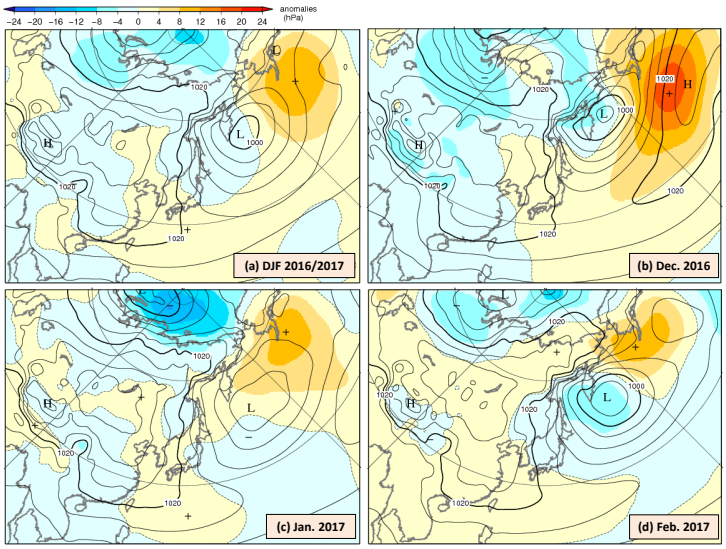


**Figure 23 Sea level pressure (a) averaged over the three months from December 2016 to February 2017, for (b) December 2016, (c) January 2017 and (d) February 2017**

The contours indicate sea level pressure at intervals of 4 hPa, and the shading shows related anomalies. H and L indicate the centers of high and low pressure systems, respectively, and + (plus) and – (minus) show the peak and bottom of sea level pressure anomalies, respectively.

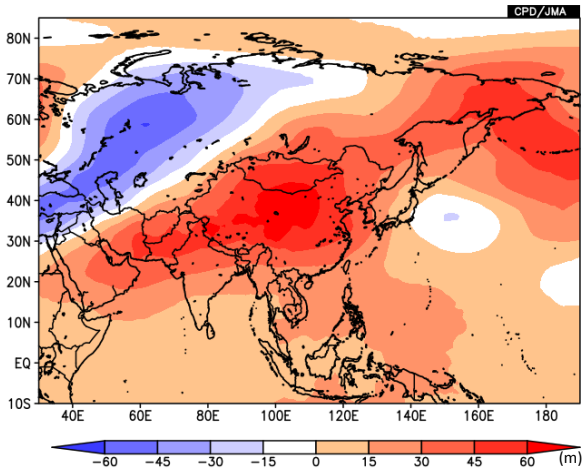


**Figure 24 Three-month mean anomalies of 300 – 850-hPa height difference for December 2016 to February 2017**

Positive values indicate higher-than-normal tropospheric temperatures.

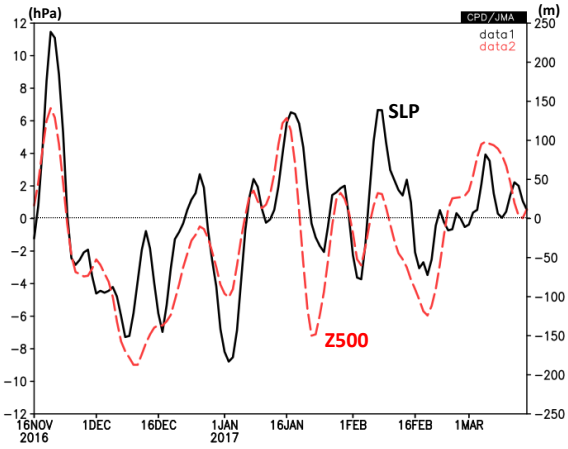


**Figure 25 Intraseasonal variation of area-averaged sea level pressure anomalies around the center of the Siberian High (40 – 60°N, 80 – 120°E; black; left axis) and 500-hPa height anomalies around Western Siberia (50 – 80°N, 50 – 90°E; red; right axis) from 16 November 2016 to 15 March 2017**

Lines indicate five-day running means.

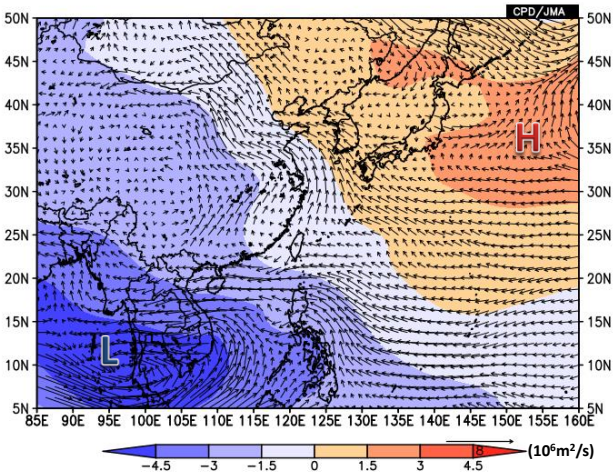


**Figure 26 850-hPa wind anomalies (arrows) and 850-hPa stream function anomalies (shading) for 1 December 2016 to 10 January 2017**

H and L denote the centers of anticyclonic and cyclonic circulation anomalies, respectively.

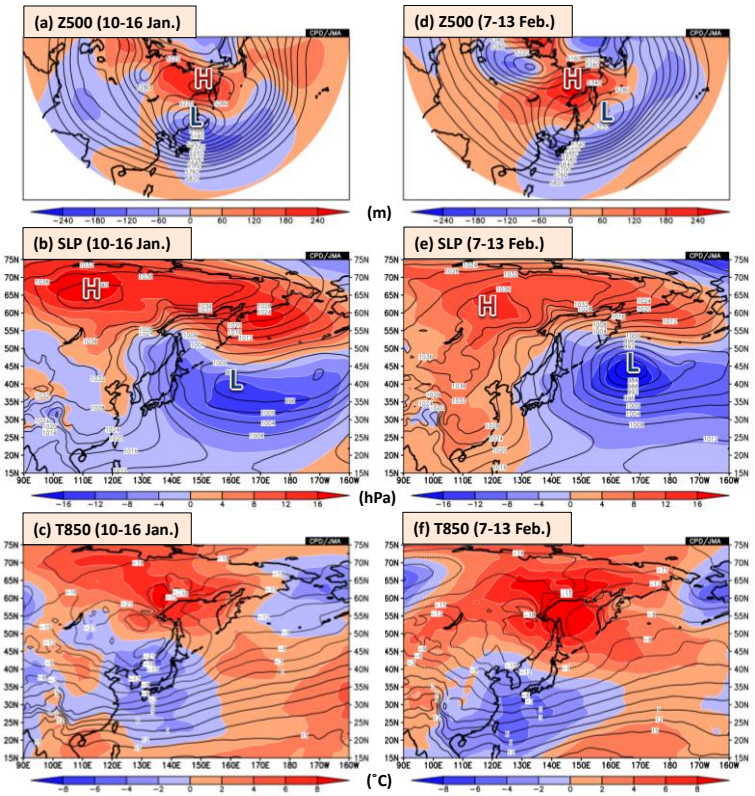


**Figure 27 ((a), (d)) 500-hPa height, ((b), (e)) sea level pressure and ((c), (f)) 850-hPa temperature for ((a) – (c)) 10 – 16 January and ((d) – (f)) 7 – 13 February 2017**

Contours indicate seven-day mean values at intervals of ((a), (d)) 60 m, ((b), (e)) 4 hPa and ((c), (f)) 3°C, and shading denotes related anomalies.

**References**

Ishii, M., A. Shouji, S. Sugimoto and T. Matsumoto, 2005: Objective Analyses of Sea-Surface Temperature and Marine Meteorological Variables for the 20th Century using ICOADS and the Kobe Collection. Int. *J. Climatol*., **25**, 865-879.

Kobayashi, S., Y. Ota, Y. Harada, A. Ebita, M. Moriya, H. Onoda, K. Onogi, H. Kamahori, C. Kobayashi, H. Endo, K. Miyaoka, and K. Takahashi, 2015: The JRA-55 Reanalysis: General Specifications and Basic Characteristics. *J. Meteorol. Soc. Japan*, **93**, 5 – 48.

## TCC contributions to Regional Climate Outlook Forums in Asia

**WMO Regional Climate Outlook Forums (RCOFs) bring together national, regional and international climate experts on an operational basis to produce regional climate outlooks based on input from participating NMHSs, regional institutions, Regional Climate Centers and global producers of climate predictions. By providing a platform for countries with similar climatological characteristics to discuss related matters, these forums ensure consistency in terms of access to and interpretation of climate information. In spring 2016, TCC experts participated in two RCOFs in Asia.**

### FOCRA II

The first RCOF was held at the 13th session of the Forum on Regional Climate Monitoring, Assessment and Prediction for Regional Association II (FOCRA II) in Beijing, China, from 24 to 26 April. At the event, experts from 16 countries/territories made presentations in seven sessions featuring talks by invited lecturers and other oral presentations. TCC attendees gave two presentations outlining the details of the last winter monsoon and the outlook for this summer based on JMA's seasonal Ensemble Prediction System. The presentations contributed to discussions on a consensus outlook for the coming summer.


Masayuki Hirai presents JMA's seasonal forecast at FOCRA II.

### SASCOF-10

The second RCOF was the tenth session of the South Asian Climate Outlook Forum (SASCOF-10) held in Thimphu, Bhutan, from 24 to 26 April. This forum has been held every year since 2010 to provide a consensus outlook for South Asian monsoon season. The member countries are Afghanistan, Bangladesh, Bhutan, India, Maldives, Myanmar, Nepal, Pakistan and Sri Lanka. The SASCOF consensus outlook is critically important in efforts by these nations to prevent disasters caused by extreme climate events such as heavy rainfall and droughts. Experts from member countries share outlooks for their own countries and engage in discussions with experts from global centers to formulate a consensus outlook. As a contribution to such activities, TCC dispatches experts annually to provide the latest South Asian monsoon prediction based on JMA's seasonal Ensemble Prediction System (EPS) and to contribute to discussions on the consensus outlook.

Two TCC experts participated in SASCOF-10 to provide predictions on oceanic and atmospheric conditions, including probabilistic forecasting of monsoon rainfall in South Asia based on JMA's seasonal EPS, and briefly outlined the Center's services. The prediction was consistent with those based on other models and supported a decision on the outlook for the 2017 summer monsoon season.


Takashi Yamada presents JMA's seasonal forecast (top) and Yasushi Mochizuki presents TCC's activities (bottom) at SASCOF-10.

**Short note from a TCC expert – meeting with Bhutan NMHS staff**

As no TCC staff have yet had an opportunity to visit Bhutan's National Center for Hydrology and Meteorology (NCHM), TCC and NCHM representatives met cordially on the sidelines of SASCOF-10. The NCHM staff highlighted the current status of their operational climate activities, and possible future collaborative work was discussed. This was fruitful as a TCC focal point in clarifying how NCHM staff provide climate services to national users and in understanding the current status of such services.

The RCOF provides valuable opportunities for TCC, in its role as a Regional Climate Center, to interact directly with users engaging in climate activities with TCC products and to collect related feedback. Such input contributes significantly to the improvement of TCC products and activities.

TCC sincerely appreciates the contribution of the relevant NCHM representatives to these fruitful discussions.

*(FOCRA II: Masayuki Hirai and Shingo Ito, SASCOF-10: Takashi Yamada and Yasushi Mochizuki Tokyo Climate Center)*

## TCC Experts Visit Indonesia

TCC arranges expert visits to NMHSs to support capacity building for climate services and facilitate the effective transfer of technical expertise on TCC products and tools.

As part of such efforts, two TCC experts visited the Meteorological, Climatological, and Geophysical Agency of Indonesia (BMKG) from 21 to 23 March 2017 to hold a training seminar on the generation of climate analysis information with focus on statistical and dynamical relationships between primary modes of global-scale climate variability and regional/local climates in the target country. The training was also intended to promote the effective use of TCC's Interactive Tool for Analysis of the Climate System (iTacs). The visit was conducted as follow-up to the 2016 TCC Training Seminar (see TCC News No. 46 and the TCC website for details), and provided a valuable platform for discussions on future collaboration between BMKG and TCC.

With the attendance of around 20 staff from regional branches of BMKG and a dozen from its headquarters, the TCC trainers began with a practice session for basic iTacs operation. On the second day, presentations were given on expertise and techniques necessary to identify the statistical relationship between temperature and precipitation in Indonesia and primary modes of global climate variability, such as El Niño-Southern Oscillation (ENSO) and the Indian Ocean Dipole (IOD) Mode. The trainers then outlined how to interpret statistical results from the viewpoint of climatological and meteorological dynamics. Using this background expertise and the TCC analysis tool (available via the TCC website), the attendees worked hard to produce climate analysis information for their regions in Indonesia and gave presentations on their achievements. Another significant outcome of the seminar was the advanced iTacs operation expertise gained by the attendees.

The visit provided outstanding opportunities for both TCC and BMKG. The attendees deepened their understanding of primary modes and their expected impacts on the regional climate of Indonesia, and TCC staff enjoyed fruitful discussions on future collaboration with BMKG. TCC will continue to arrange expert visits to NMHSs in Southeast Asia and elsewhere as necessary to assist with operational climate services.

*(Yoshinori Oikawa and Yasushi Mochizuki, Tokyo Climate Center)*

You can also find the latest newsletter from Japan International Cooperation Agency (JICA).

**JICA's World (April 2017)**
https://www.jica.go.jp/english/publications/j-world/c8h0vm0000b2tu4r-att/1704.pdf
JICA's World is the quarterly magazine published by JICA. It introduces various cooperation projects and partners along with the featured theme. The latest issue features "The Gaining Ground: The Bright Future of Asia and the Pacific".

Any comments or inquiry on this newsletter and/or the TCC website would be much appreciated. Please e-mail to tcc@met.kishou.go.jp.

(Editors: Kiyotoshi Takahashi, Yasushi Mochizuki and Atsushi Minami)

Tokyo Climate Center (TCC), Japan Meteorological Agency
Address: 1-3-4 Otemachi, Chiyoda-ku, Tokyo 100-8122, Japan
TCC Website: http://ds.data.jma.go.jp/tcc/tcc/index.html